ENVIRONMETRICS
Environmetrics 2001; **12**: 401–420 (DOI: 10.1002/env.462)

Assessment of regional air pollution variability in Istanbul

Zekai Şen[1*] and Ahmet Öztopal[2]

[1]*Civil Engineering Faculty, Hydraulics Division, Istanbul Technical University, Maslak 80626, Istanbul, Turkey*
[2]*Department of Meteorology, Atmospheric Environment Group, Istanbul Technical University, Maslak 80626, Istanbul, Turkey*

SUMMARY

Air pollution concentrations have temporal and spatial variations depending on the prevailing weather conditions, topographic features, city building heights and locations. When the measurements of air pollutants are available at set measurement sites, the regional variability degree of air pollutants is quantified using the point cumulative semi-variogram (PCSV). This technique provides a systematic method for calculating the changes in the concentrations of air pollutants with distance from a specific site. Regional variations of sulphur dioxide (SO_2) and total suspended particulate (TSP) matter concentrations in Istanbul city were evaluated using the PCSV concept. The data were available from 16 different air pollution measurement stations scattered all over the city for a period from 1988 to 1994. Monthly regional variation maps were drawn in and around the city at different radii of influence. These maps provide a reference for measuring future changes of air pollution in the city.

KEY WORDS: air pollution; point cumulative semi-variogram; regionalization; radius of influence; sulphur dioxide; total suspended particulate; variability degree

1. INTRODUCTION

The atmospheric boundary layer is polluted due to industrialization, population increase and transportation activities, particularly during the winter months due to heating by burning fossil fuels that releases emissions into the atmosphere. This is a major health risk to the residents of large cities where the problem is more serious and more complex because of the irregular construction of buildings and their associated heat island effects. Local and temporal restrictions at the time of air pollution occurrences are insufficient and temporary with margional benefits. It is, therefore, necessary to establish a scientific approach to collect systematic air pollutant measurements and to extract the information from them so decisions can be made on sound foundations.

The most difficult aspect in the systematic assessment of air pollution is the selection of the locations of measurement stations, so that regional variability can be adequately estimated. Historical information and expert opinions should be used for the allocation of sampling sites. Given the sampling network, several questions (Şen; 1995) are often asked, such as:

1. How to quantify, from limited and irregular site measurements, the regional air pollution distribution?

*Correspondence to: Z. Şen, Civil Engineering Faculty, Hydraulics Division, Istanbul Technical University, Maslak 80626, Istanbul, Turkey. E-mail: zsen@itu.edu.tr

Received 11 November 1999
Accepted 21 August 2000

2. How to model the changes over the area of interest?
3. How to construct maps reflecting the degrees of regional variability?

Almost all the efforts of the majority of researchers have been directed at the modelling of air pollution at a single location, particularly using univariate time series methods (Larsen, 1971; Merz *et al.*, 1972; Chock *et al.*, 1975; Zinsmeister and Redman, 1980; Taylor, 1915; Taylor *et al.*, 1986). Such efforts are incapable of providing regional information on the air pollutants' spatial variations, they are only suitable for providing temporal knowledge for the measurement sites. On the other hand, a few researchers have focused on modelling the spatial pattern using methods that require an involved mathematical background and a vast amount of data (Melli *et al.*, 1981; Haslett and Raftery, 1989). Perhaps the most frequently used approach to display spatial variations of air pollutants is through hand-drawn maps. Other researchers have used data reduction methods, particularly principal component analysis (Peterson, 1970, 1972; Henry and Hidy, 1979) to summarize the regional variation in air pollution.

Şen (1995) proposed the use of a cumulative semi-variogram (CSV) technique for evaluating qualitatively the regional features of air pollution concentration and dispersion. Here this method is implemented for two air pollutants (SO_2 and total suspended particulate (TSP) in the city of Istanbul. These two pollutants are measured most frequently on a regional scale at different sites in and around the city centre. Also, under favourable weather conditions these pollutants occur in high concentrations and their mean daily and monthly concentrations at several stations become higher than air quality standards at many instances during the winter season. Recently, Anh *et al.* (1997) used CSV to estimate the regional dependence or air pollutants for Sydney in Australia. The average radius of influence was determined as 17 km for this city. However, a constant radius of influence is not reliable because it should also depend on the variation or the meteorological conditions.

2. POINT CUMULATIVE SEMI-VARIOGRAM METHOD

The classical semi-variogram (SV) was defined by Matheron (1963) for measuring spatial dependence for irregularly sampled sites. Let $C_1, C_2, \ldots, C_m$ be the measured concentrations at m sites in the area of interest, and let d_{jl} be the distance between site j and l. Then, SV at distance d is defined as (Clark, 1979; Journal and Huijbregts, 1978; Isaaks and Srivastava, 1989)

$$\gamma_d = \frac{1}{2N_d}\sum_{i=1}^{N_d}(C_i - C_i(d))^2 \tag{1}$$

where N_d is the number of d equally spaced sites. The point cumulative semi-variogram (PCSV) was proposed by Şen (1989) as an extension of the ordinary SV and for use in earth sciences. PCSV attempts to measure the spatial variability around a site. In other words, it gives the regional effect of all other sites within the area on the site of concern. Let C_e be the concentration at the site of interest e and let $d_{e1}, d_{e2}, \ldots, d_{e(m-1)}$ be the ordered distances of site e from the remaining $(m-1)$ sites. Then the PCSV of e at distance d is defined as

$$\gamma_e(d) = \frac{1}{2}\sum_{d_{ei}<q_d}(C_e - C(d_{ei}))^2 \tag{2}$$

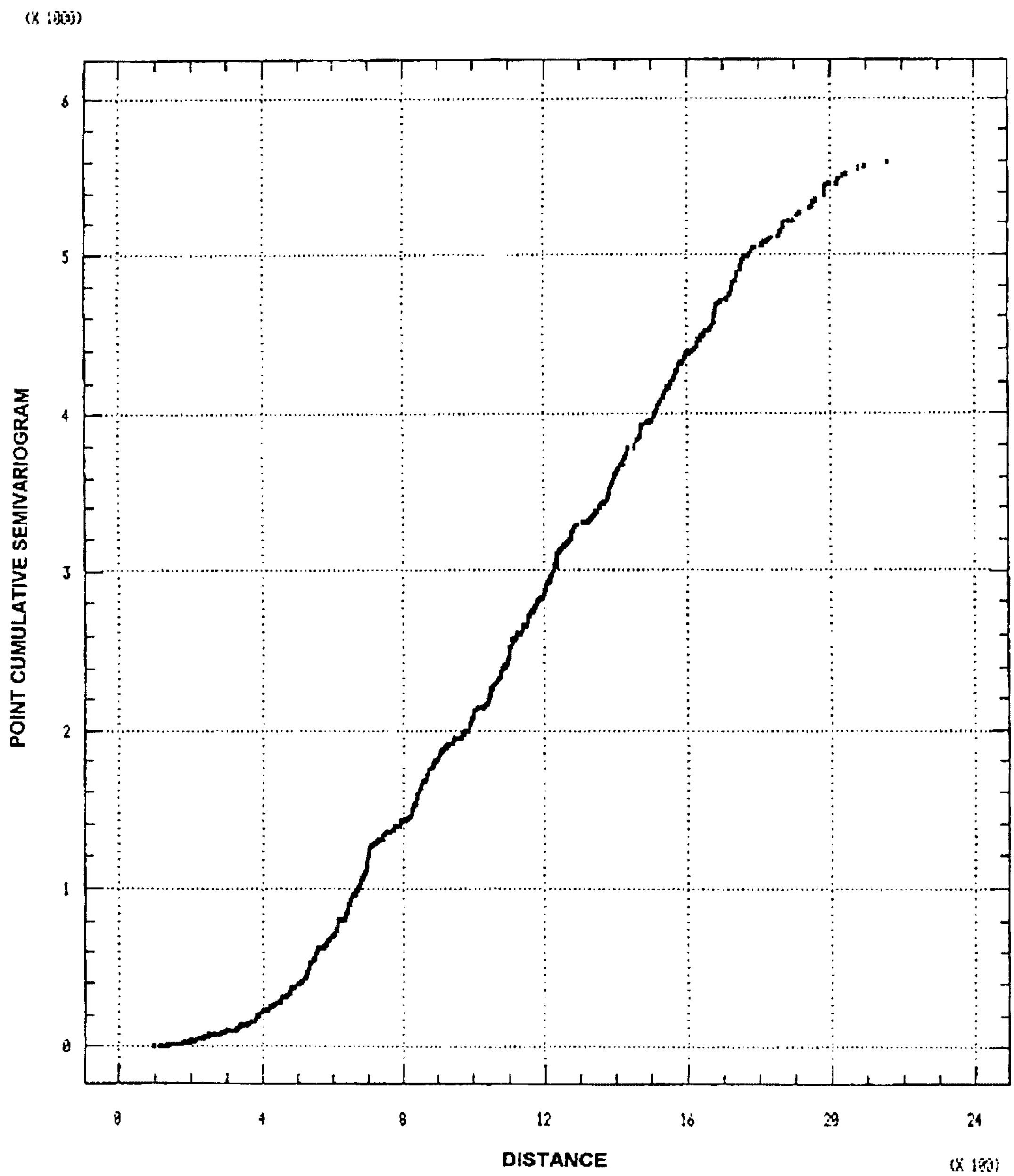

Figure 1. Sample PCSV

Figure 1 gives the plot of $\gamma_e(d)$ versus d. This can be done for each site which results in m sample PCSV curves. Note that no *a priori* selection of distance classes is required for computing PCSV as is commonly used when calculating SV. The PCSV provides information on sources for the site of interest and helps in defining the radius of influence and structural behaviour of regionalized variables near the site.

3. FEATURES OF THE STUDY AREA AND DATA

The Istanbul city metropolitan area is situated around the location, latitude 41°N, longitude 29°E at the north-western corner of Turkey, as shown in Figure 2. This historical city has expanded on an unexpected scale in both industrialization and population during the past two decades. Consequently, the local and central authorities have faced many environmental problems, such as air, land and water

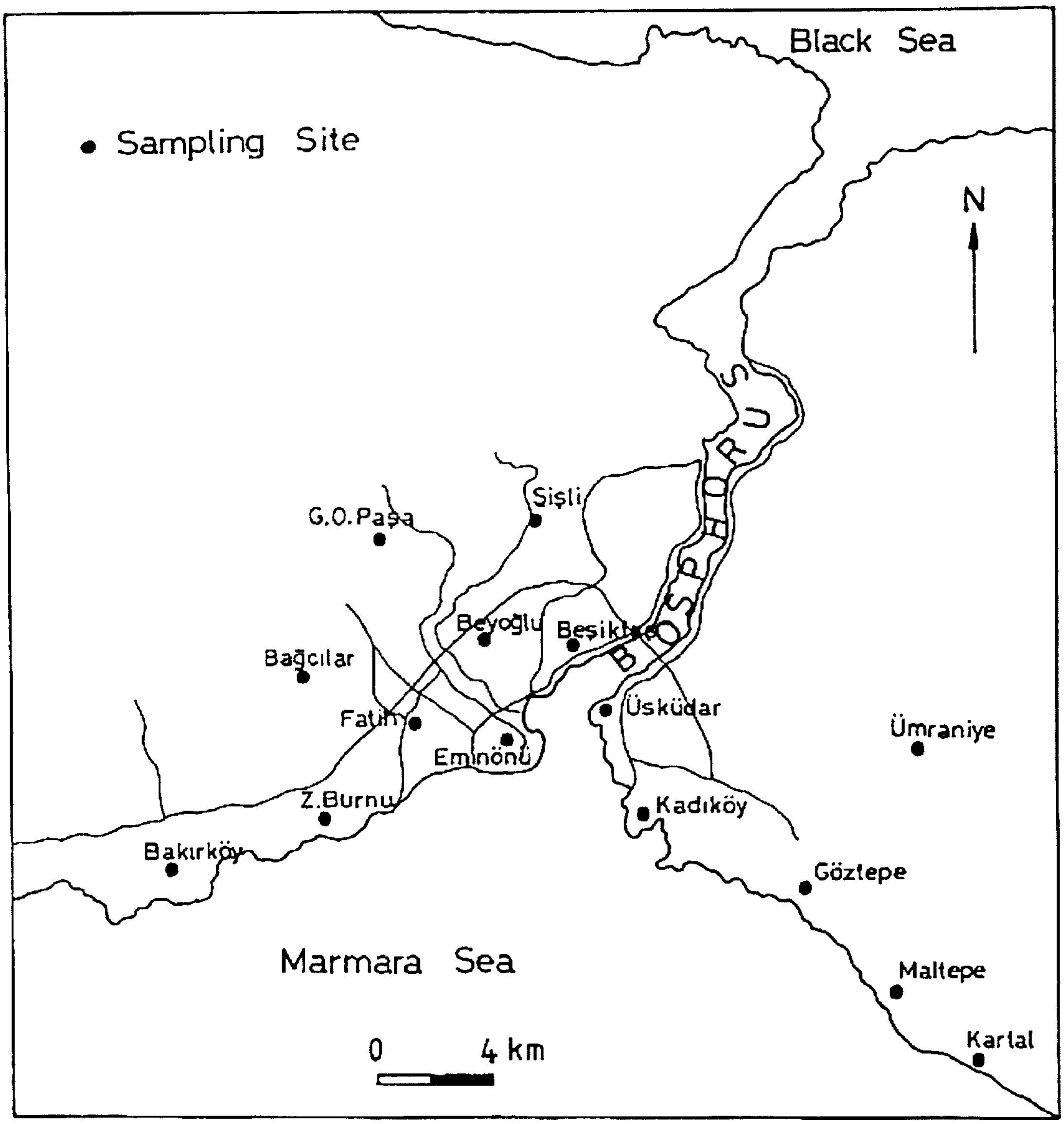

Figure 2. Location map

Table I. İstanbul air pollution monitoring station characteristics

Station name	Continent	Longitude (N)	Latitude (E)	Averages (ppm)		Standard deviation (ppm)	
				SO_2	TSP	SO_2	TSP
Göztepe	Asia	29.055°	40.977°	218.73	60.09	172.30	32.37
Ümraniye	Asia	29.091°	41.029°	140.45	55.09	86.21	27.14
Kadiköy	Asia	29.024°	41.001°	122.09	52.00	73.77	42.85
Üsküdar	Asia	29.021°	41.020°	135.91	56.54	78.90	25.55
Maltepe	Asia	29.136°	40.932°	110.64	58.91	66.16	24.88
Kartal	Asia	29.173°	40.917°	87.00	59.09	35.57	19.81
Eminönü	Europe	28.976°	41.011°	167.36	89.45	121.90	47.26
Şişli	Europe	28.989°	41.058°	198.64	63.54	156.50	35.16
Beyoğlu;	Europe	28.982°	41.033°	174.09	72.45	115.50	38.11
Fatih	Europe	28.941°	41.026°	172.54	81.91	139.70	42.24
G.O.P	Europe	28.911°	41.059°	189.36	102.73	131.10	53.49
Bakirköy	Europe	28.865°	40.994°	164.73	82.82	111.90	30.85
Bağcilar	Europe	28.853°	41.054°	144.82	87.45	94.48	26.52
Beşiktaş	Europe	29.008°	41.053°	156.09	79.91	94.14	33.01
Zeytinburnu	Europe	28.917°	41.005°	129.54	60.64	72.02	28.08
Bayrampaşa	Europe	28.903°	41.042°	161.11	103.11	96.53	33.56

pollution. At time, air pollution episodes with favouring meteorological conditions surpass WHO standards, as shown by Incecik(1996).

The SO_2 records are actual measurements of the gaseous acidity of the air and an acidimetric titration method is used for its measurement. The air sample is labelled through a dilute hydrogen peroxide solution where SO_2 is absorbed and oxidized to form H_2SO_4 and the results are related to sulphur dioxide concentration in the sample. On the other hand, TSP is measured by a filter soiling method. The darkness of the stain is converted to a concentration value. The measurements at each site are obtained by the same instruments and the same calibration procedures.

Currently, there are 16 air pollution monitoring stations established to measure SO_2 and TSP concentrations within the atmospheric boundary layer over Istanbul. These stations are scattered on the European and Asian sides of the city as shown in Figure 2. Table I gives the location of the sites and some of their statistical features. Six of these stations are located on the Asian side where the air pollution level is lower than that on the European side. Historical expansions have taken place on the Marmara seacoast in the south (Figure 2). Table I gives the mean and standard deviation of SO_2 and TSP. The average SO_2 for stations on the Asian side is 135.8 ppm whereas that on the European side is 165.82 ppm. This shows that the European side is more polluted. TSP shows the same pattern. It should also be noted that the average standard deviation is higher on the European side.

Table II gives the monthly averages at each station for the two pollutants with SO_2 in the first line and TSP in the second line. Since, there is no air pollution problem in August it is not included in the table. It is obvious that high pollutant levels occur in the winter months.

4. PCSV INTERPRETATIONS

Radius of influence determination is a difficult problem in meteorology (Cressman, 1959; Sasaki, 1960; Barnes, 1964). It is defined as the radius of a circle that contains all locations that influence

Table II. Monthly averages of SO_2 and TSP concentrations

Stations	Months									
	January	February	March	April	May	June	July	September	October	November	December
Göztepe	542	386	340	141	57	49	41	75	82	261	432
	112	*101*	*62*	*44*	*37*	*30*	*19*	*27*	*42*	*86*	*101*
Ümraniye	226	234	238	112	63	36	49	80	61	166	280
	92	*76*	*56*	*48*	*45*	*31*	*16*	*25*	*39*	*72*	*106*
Kadiköy	243	209	129	102	81	78	58	63	55	67	258
	121	*85*	*16*	*16*	*23*	*26*	*20*	*18*	*115*	*23*	*109*
Üsküdar	256	196	199	125	67	53	44	77	65	144	269
	109	*88*	*53*	*45*	*47*	*37*	*24*	*32*	*37*	*68*	*82*
Maltepe	222	173	180	86	54	53	27	61	56	108	197
	111	*85*	*64*	*48*	*53*	*41*	*27*	*31*	*37*	*69*	*82*
Kartal	161	127	116	77	51	71	37	54	68	88	107
	95	*74*	*53*	*57*	*62*	*51*	*31*	*39*	*36*	*62*	*90*
Eminönü	316	237	209	114	66	68	63	74	81	155	458
	148	*121*	*88*	*64*	*54*	*45*	*40*	*49*	*64*	*118*	*193*
Ş işli	400	346	361	134	88	57	49	46	48	182	474
	111	*97*	*85*	*43*	*48*	*26*	*17*	*27*	*41*	*83*	*121*
Beyoğlu	319	347	270	123	93	64	58	67	73	154	347
	134	*120*	*115*	*49*	*54*	*34*	*22*	*34*	*55*	*70*	*110*
Fatih	350	398	326	117	59	45	33	44	45	154	327
	143	*122*	*114*	*61*	*51*	*36*	*25*	*33*	*66*	*116*	*134*
G.O.P	344	372	336	110	88	132	42	40	42	238	339
	182	*123*	*95*	*53*	*80*	*78*	*20*	*39*	*192*	*122*	*146*
Bakirköy	340	332	261	123	67	51	50	60	64	199	265
	147	*101*	*90*	*69*	*70*	*44*	*42*	*58*	*72*	*96*	*122*
Bağcilar	281	242	227	130	122	51	40	33	46	133	288
	129	*111*	*88*	*65*	*100*	*55*	*46*	*63*	*79*	*108*	*118*
Beşiktaş	299	289	246	129	77	59	52	73	70	169	254
	115	*99*	*96*	*65*	*70*	*52*	*38*	*38*	*58*	*100*	*148*
Zeytinbur.	243	217	212	99	72	58	49	67	58	156	194
	116	*87*	*69*	*43*	*51*	*31*	*26*	*27*	*49*	*83*	*85*
Bayramp.	–	329	307	155	105	70	66	87	101	230	–
	–	*152*	*126*	*96*	*103*	*80*	*75*	*51*	*88*	*157*	–

the location of interest. It is well known that as the distance from the location increases, the dependence decreases non-linearly and reaches a point at which this dependence disappears altogether. Plotting the PCSV for the station of interest will reveal its radius of influence. Figure 3 shows the plots of some examples of PCSV for for Istanbul. From the figure it is possible to see the following:

1. For all stations, the greater the distance the greater the cumulative variogram value, indicating the decrease in the dependence between the pivot and the surrounding stations.
2 Some of the plots show parabolic patterns but others show cubic ones. The steeper the tangent of the PCSV at a point, the smaller the dependence and vice versa. The cubic pattern, as shown in Figure 3(a), indicates that after a certain distance there is another source of high pollution that causes the dependence.
3. Some PCSVs intersect the horizontal axis, which indicates that the air pollutant between the pivot site and the other nearby sites at distances less than the distance of the intersection are almost the same.

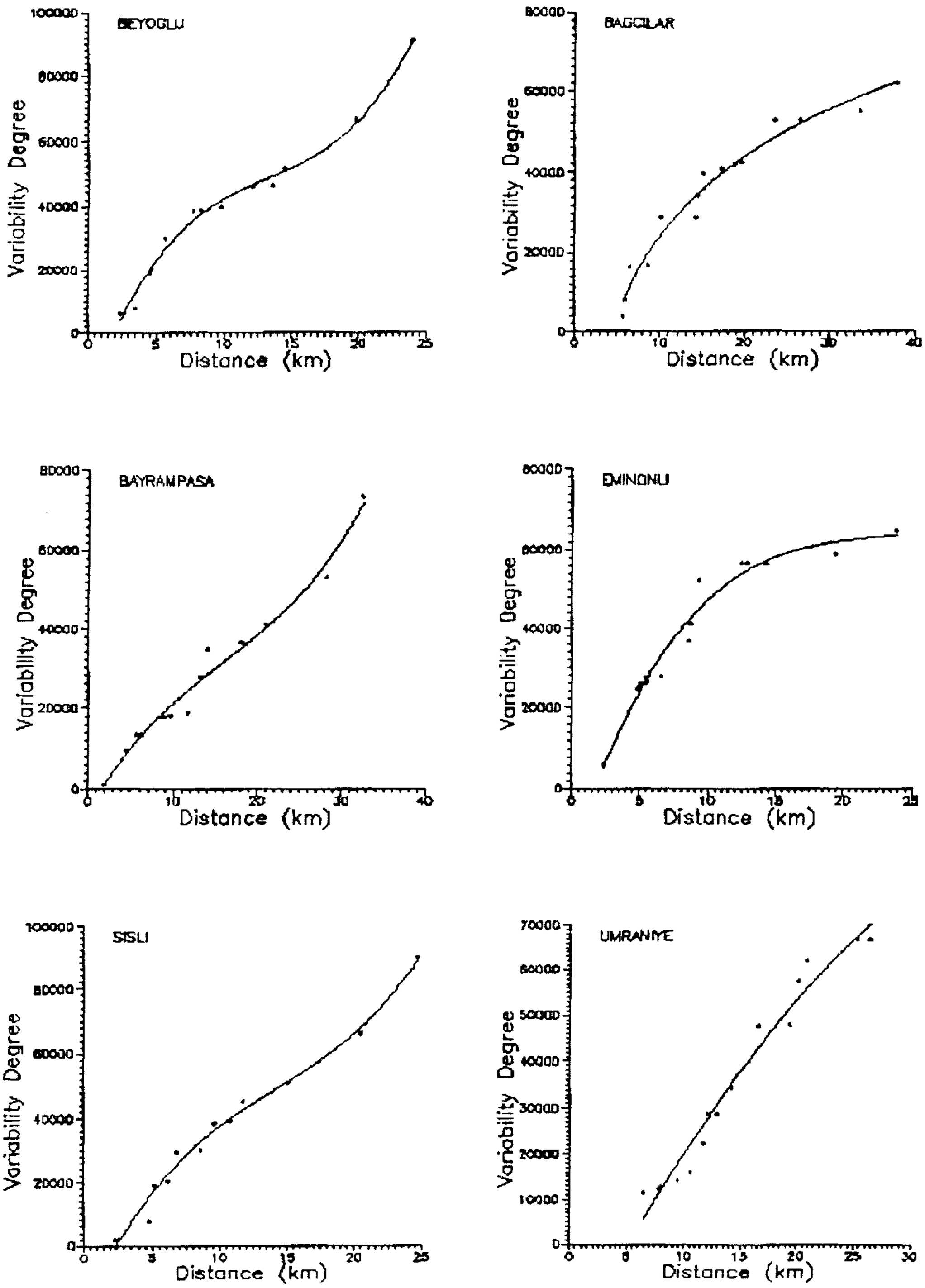

Figure 3. Sample SO_2 PCSVs at different locations for February

4. Comparisons between the PCSVs indicate that their curvatures are different from each other. The smaller the slope the less the effect of the atmospheric diffusion mechanism and the air pollutant concentrations remain constant.

5. AIR POLLUTANT VARIABILITY DEGREE MAPS

In order to show regional variability, it is possible to draw maps of PCSV values at the distances corresponding to different degrees. This gives a picture of the air pollution concentration maps at equal distances around each station. Cressman (1959) proposed, as a rule-of-thumb, using the distances 750 km, 1000 km radius of influence. Thus, three maps are used to summarize air pollution data. However, in cities like in our case, the radii of influence of air pollutants cannot be very large because the concentrations can change over a city over significantly shorter distances (20 to 25 km). In this study we chose radii of influence of 3, 5, 10, 15 and 20 km and their regional maps are provided. Here only the maps for December, January and February are presented. A detailed account and figures are available in Öztopal (1996).

Figures 4–9 show the regional SO_2 and TSP variation degree spatial distributions for December, January and February, respectively. The following interpretations can be made.

1. The existence of a straight (Bosphorus) between the Marmara and Black Seas shows a distinct effect on the regional distribution of the pollutants. The Bosphorous plays the role of a ventilation channel by allowing the passage of northerly and north-westerly wind systems that are created because of the Icelandic high-pressure centre during the winter period.
2. Pollutant concentrations are comparatively greater on the European side than on the Asian side. This may be due to various factors, such as the population is sparce on the Asian side; industrial plants are more concentrated on the European side; the Asian side is more rugged with valley-type

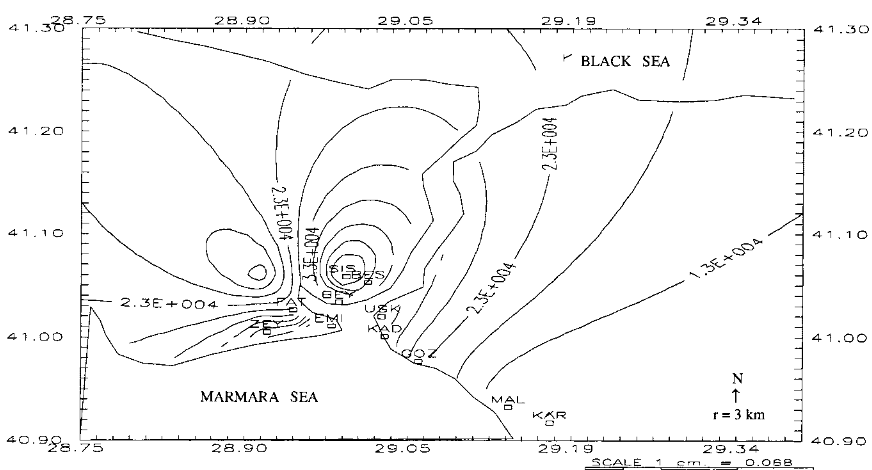

(a)

Figure 4. SO_2 regional variation maps for December at different distances

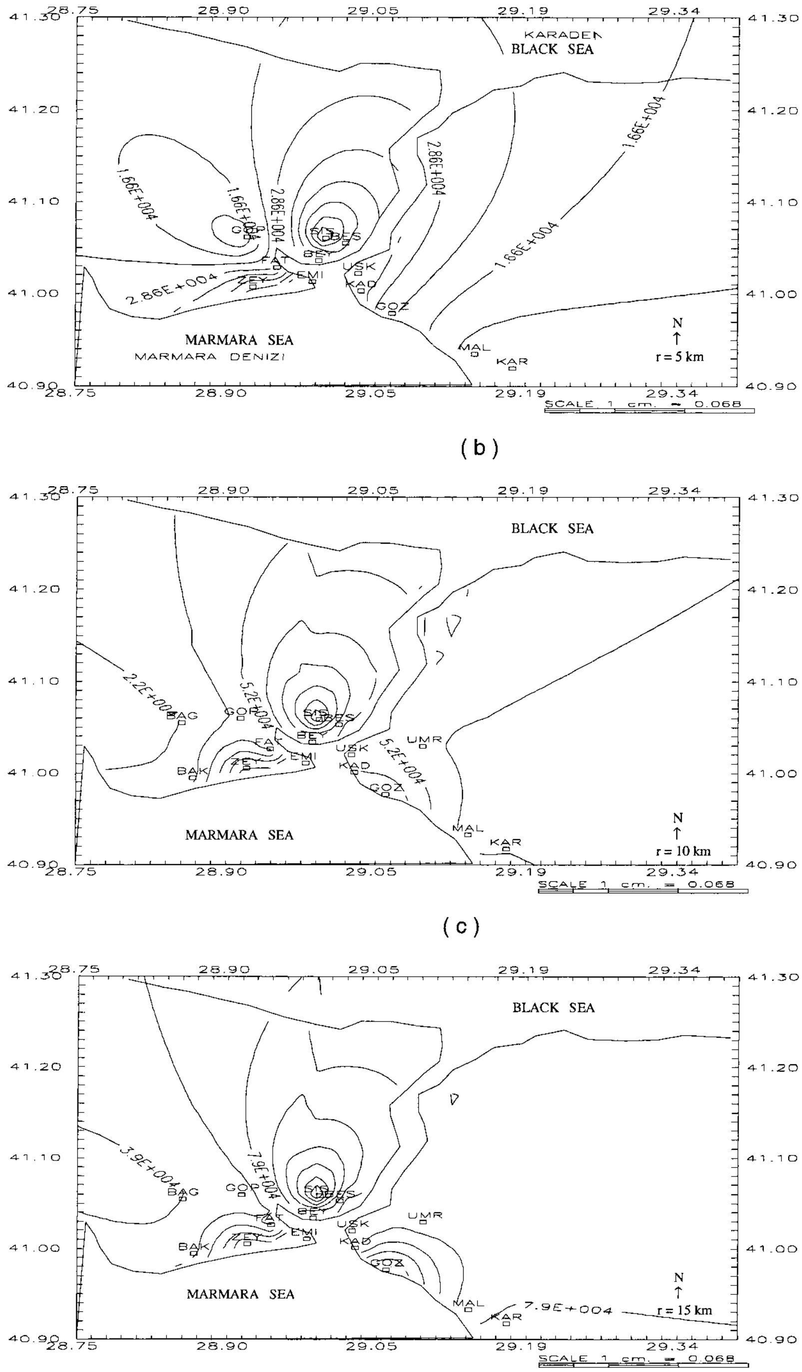

Figure 4. (*Continued*)

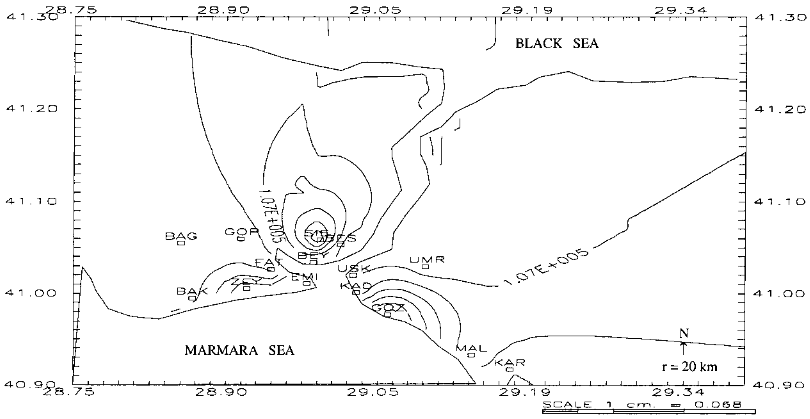

(e)

Figure 4. (*Continued*)

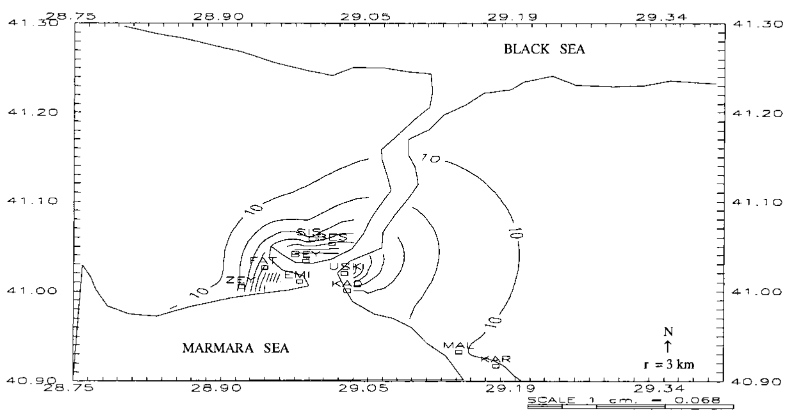

(a)

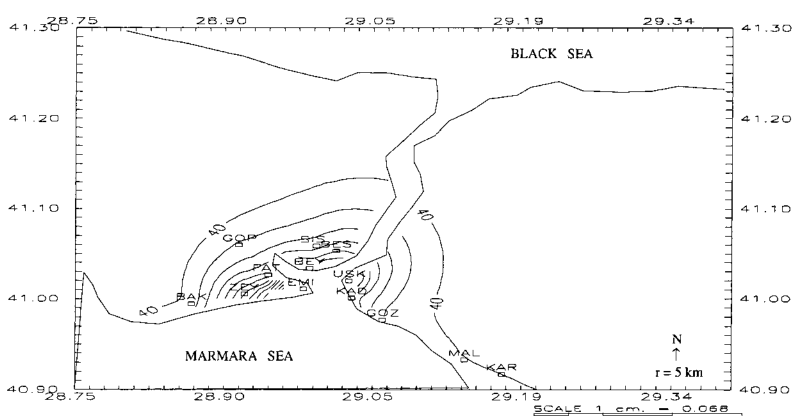

(b)

Figure 5. TSP regional variation maps for December at different distances

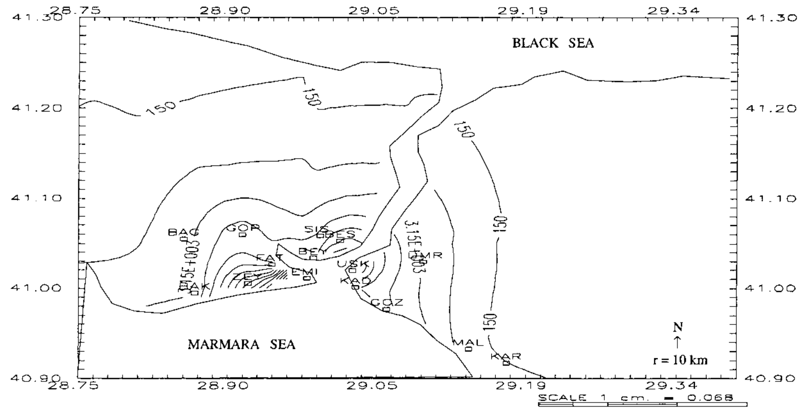

(c)

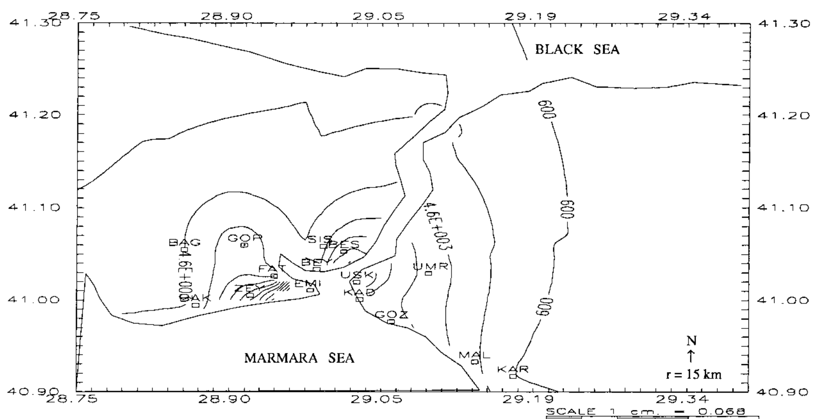

(d)

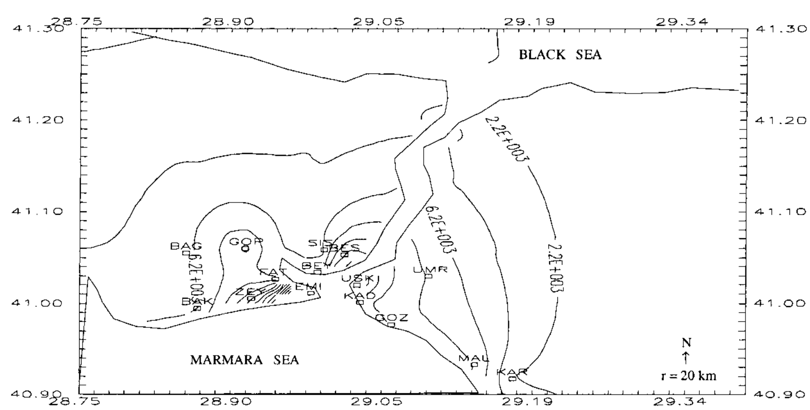

(e)

Figure 5. (*Continued*)

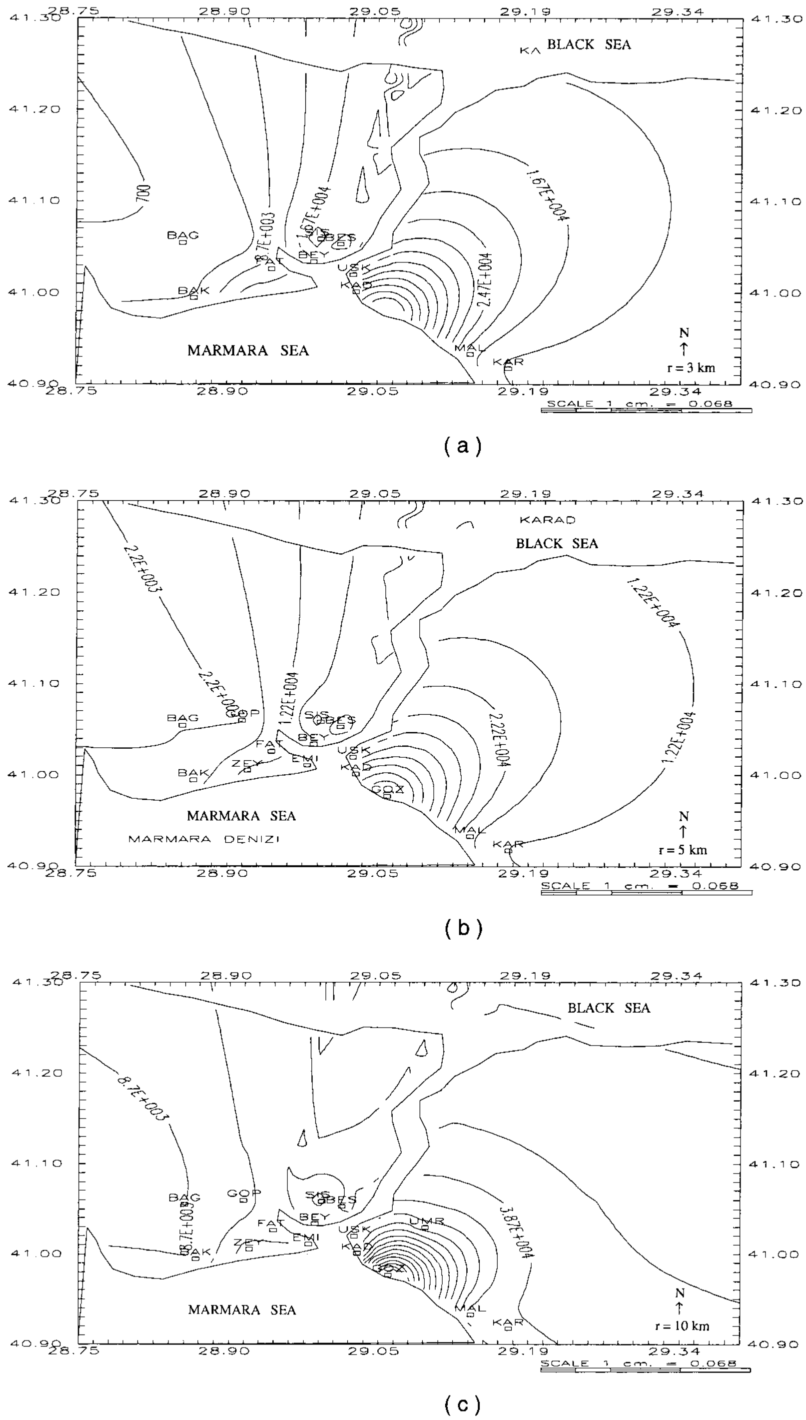

Figure 6. SO_2 regional variation maps for January at different distances

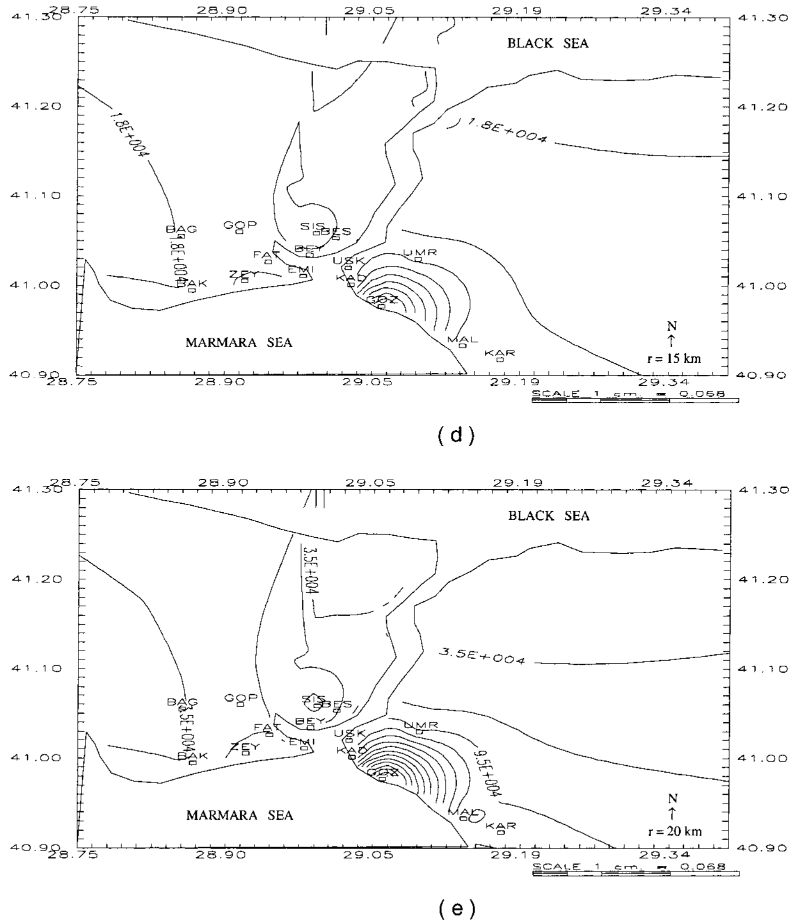

Figure 6. (*Continued*)

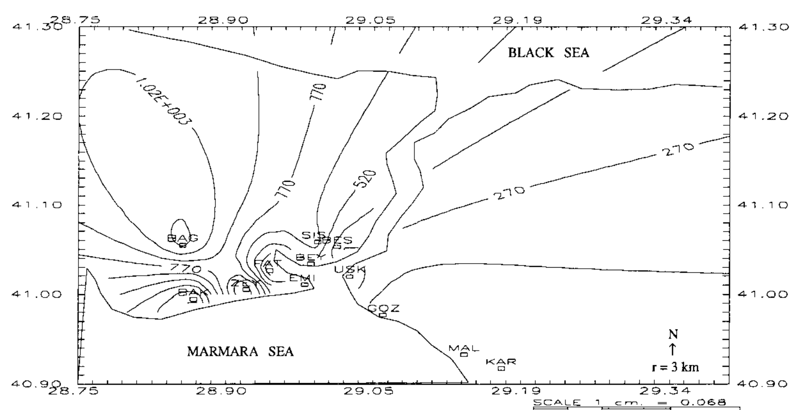

(a)

Figure 7. TSP regional variation maps for January at different distances

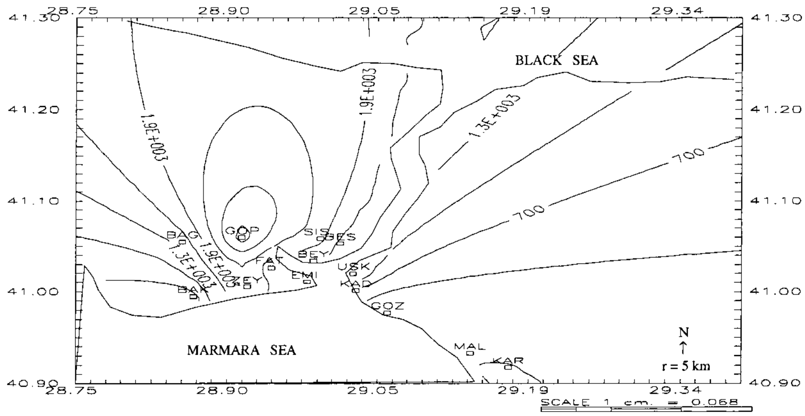

(b)

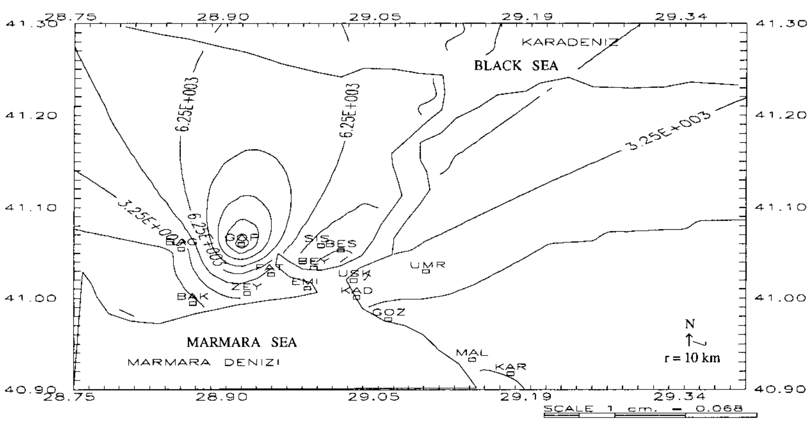

(c)

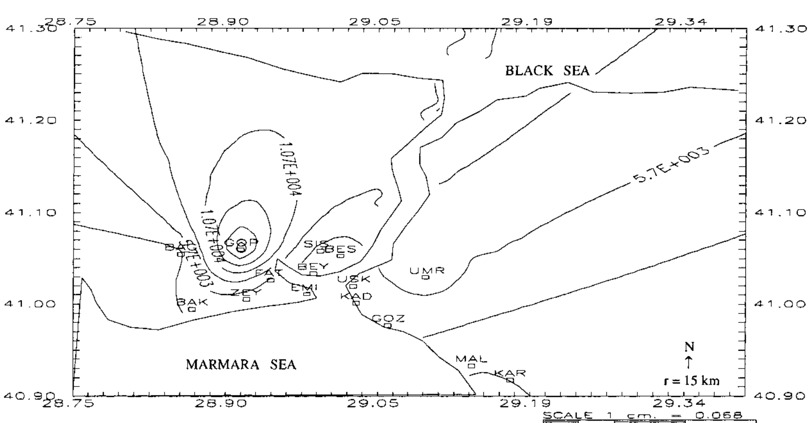

(d)

Figure 7. (*Continued*)

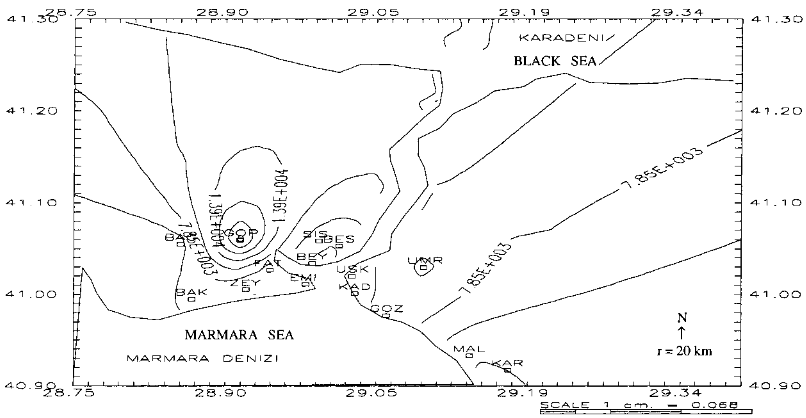

(e)

Figure 7. (*Continued*)

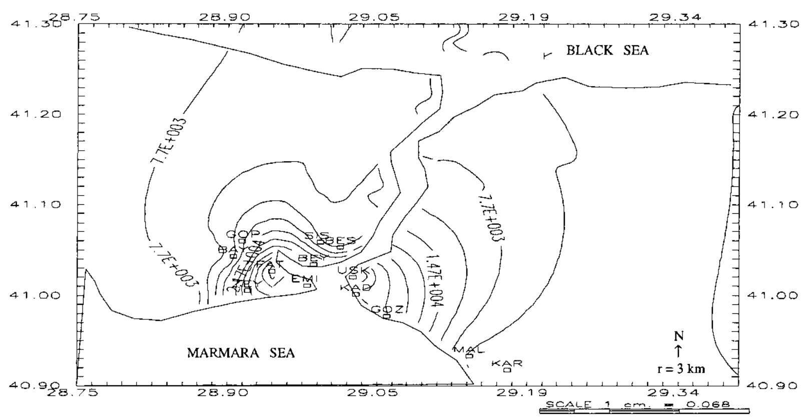

(a)

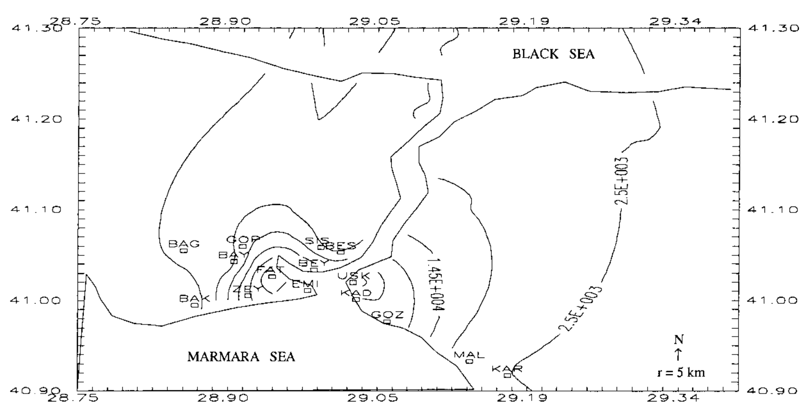

(b)

Figure 8. SO_2 regional variation maps for February at different distances

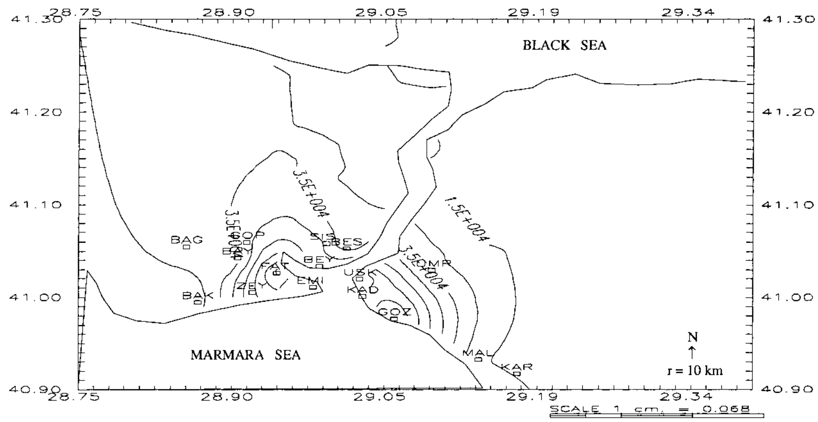

(c)

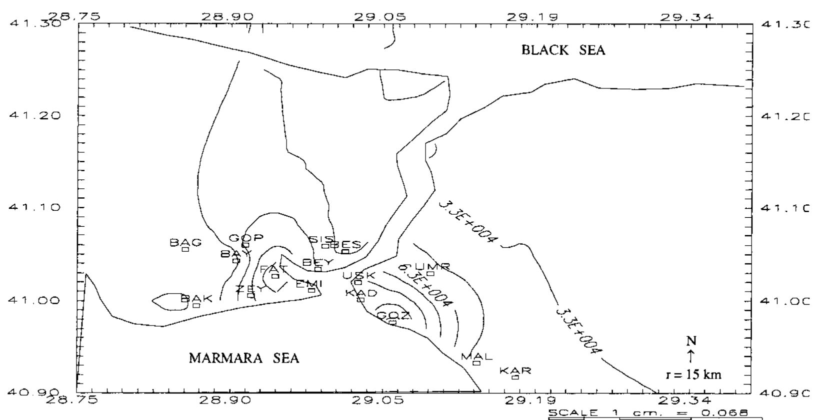

(d)

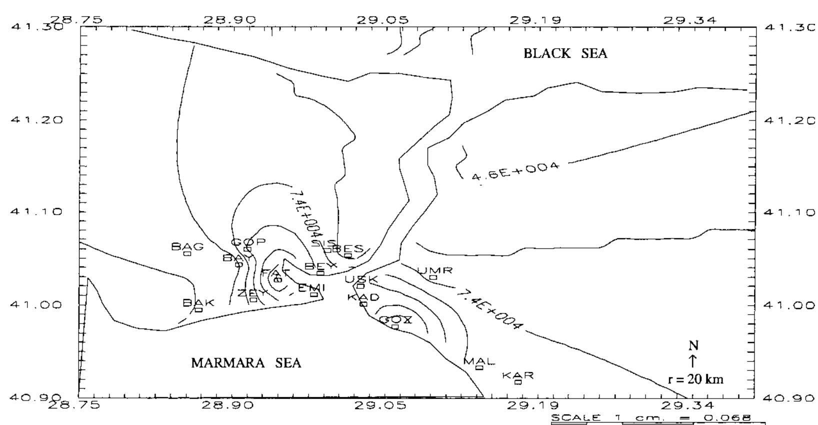

(e)

Figure 8. (*Continued*)

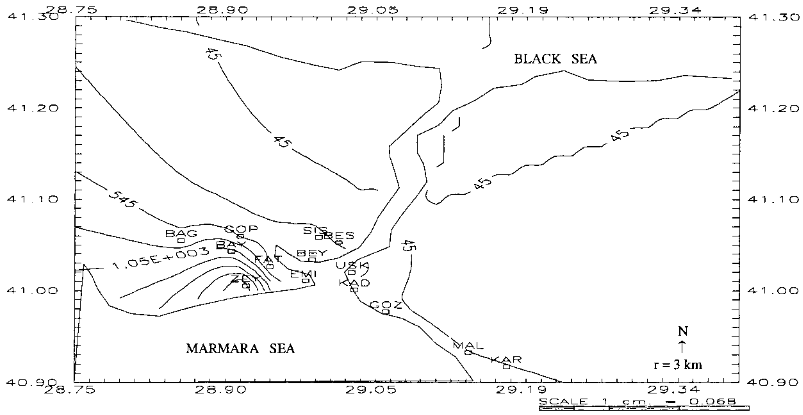

(a)

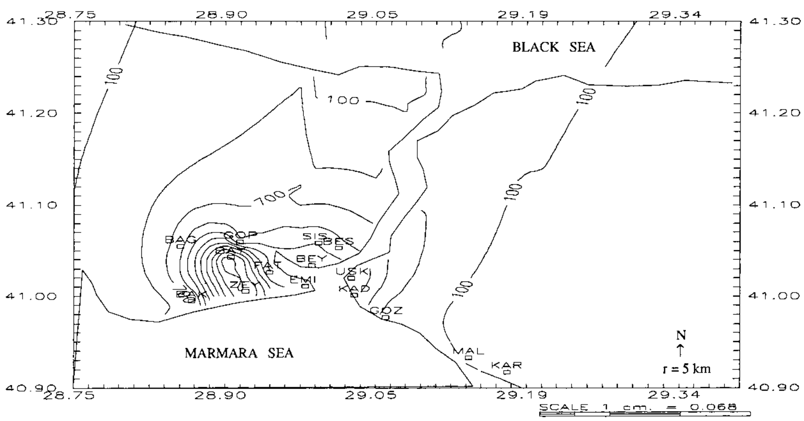

(b)

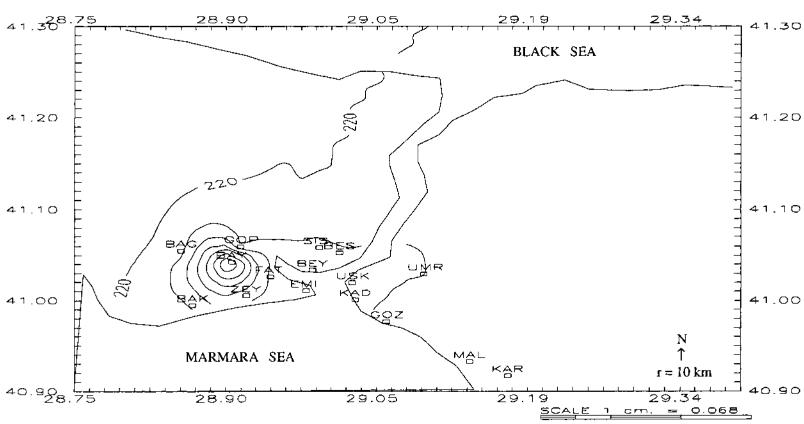

(c)

Figure 9. TSP regional variation maps for February at different distances

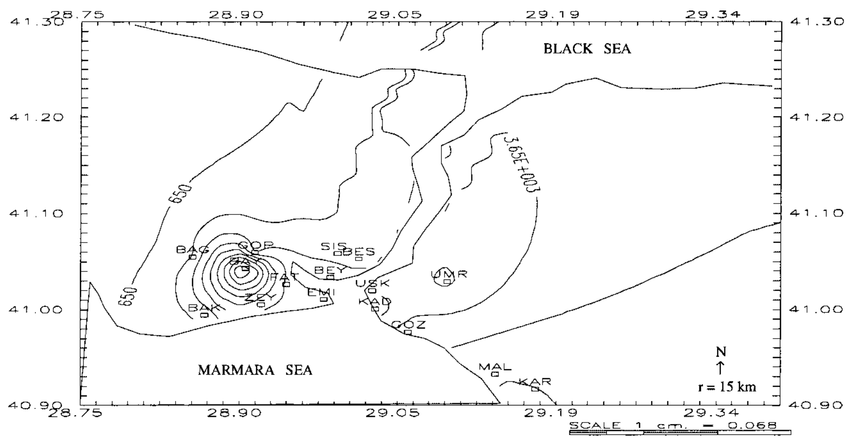

(d)

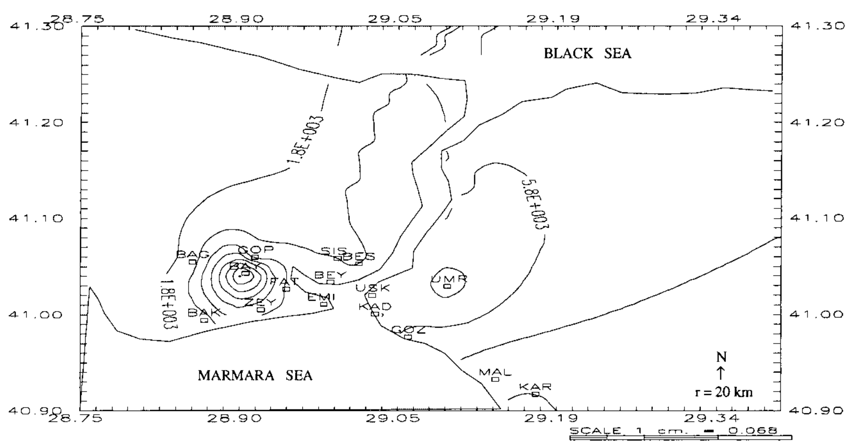

(e)

Figure 9. (*Continued*)

topographic features open to the northerly winds; and finally, the Asian side receives more rainfall than the European side.

3. The most extensive SO_2 concentrations appear at 3 km distances reaching the Black Sea coast in the north during December. In fact, at each distance, there are always highly polluted centres with closed contour lines on the European side. Such centres appear on larger distance scales (20 km) on the Asian side.
4. TSP spatial distribution maps at different distances for December, January and February are presented in Figures 5, 7 and 9, respectively. It is clear that TSP concentrations are not far dispersed but remain within and in the close vicinity of the Istanbul metropolitan area boundaries. At small distances there is no TSP transportation that reaches the Black Sea coast. In January, however, the

regional effectiveness of TSP increases and covers the whole area, but it is always under the influence of the Bosphorous ventilation channel. Local TSP concentration peaks appear in the form of closed contour lines and the locations of these centres remain the same in all maps. In February, TSP variability decreases to a point almost without closed contour lines, hence explicit TSP centres occur at small scale distances but these centres become pronounced at larger distances, especially on the European side.

6. CONCLUSION

Monthly air pollution data for the city of Istanbul have been used to show the usefulness of PCSV as a tool for determining the regional air pollution distribution. The derived maps at 3 km, 5 km, 10 km, and 20 km distances allow us to make inferences about the dispersion of SO_2 and TSP for long and short distances. One of the main objectives has been to introduce PCSV as a technique for studying spatial dependence, along with other tools used in spatial statistics.

REFERENCES

Anh V, Hiep D, Ian S. 1997. Spatial variability of Sydney air quality by cumulative semivariogram. *Atmospheric Environment* **34**: 4073–4080.

Barnes SL. 1964. A technique for maximizing details in numerical weather map analysis. *Journal of Applied Meteorology* **3**: 396–409.

Chock DP, Terrell TR, Levitt SB. 1975. Time series analysis of riverside, California air quality data. *Atomospheric Environment* **9**: 978–989.

Clark I. 1979. The semivariogram—Part 1. *Engineering Mining Journal* **180**(7): 90–94.

Cressman GP. 1959. An operational objective analysis system. *Monthly Weather Review* **87**(10): 367–374.

Davis J. 1986. *Statistics and Data Analysis in Geology*; John Wiley & Sons, Inc.: New York.

Henry RC, Hidy GM. 1979. Multivariate analysis of particulate sulfate and other air quality variables by principle components—Part I. *Atmospheric Environment* **13**: 1591–1596.

İncecik S. 1996. Investigation of atmospheric conditions in İstanbul leading to air pollution episodes. *Atmospheric Environment* **30**: 2739–2749.

Isaaks EH, Srivastava RM. 1989. *An introduction to Applied Geostatistics*; Oxford University Press: Oxford.

Journel AG, Huijbregts CI. 1978. *Mining Geostatistics*; Academic Press: London.

Larsen RL. 1971. A mathematical model for relating air quality measurements to air quality standards. Publication AP-89, Environmental Protection Agency, North Carolina.

Matheron G. 1963. Principles of geostatistics. *Economic Geology*, **58**: 1246–1266.

Melli K, Bolzern P, Franza G, Spirito A. 1981. Real-time control of sulphur dioxide emissions from an industrial area. *Atmospheric Environment* **15**: 653–666.

Merz PH, Painter LJ, Ryason PR. 1972. Aerodynamic data analysis-time series analysis and forecast and an atmospheric smog diagram. *Atmospheric Environment* **6**: 319–342.

North GR, Bell TL, Cahalan F. 1982. Sampling errors in the estimation of empirical orthogonal functions. *Monthly Weather Review* **110**: 699–706.

Öztopal A. 1996. İstanbul ilinin hava kirliliği semivariogram haritalarinin çikartilarak yorumlanmasi (Derivation of semivariogram maps for İstanbul city and their interpretations). Unpublished Thesis, İstanbul Technical University, Meteorology Department (in Turkish).

Peterson JJ. 1970. Distribution of sulfur dioxide over metropolitan St. Louis, as described by empirical eigenvectors, and its relation to meteorological parameters. *Atmospheric Environment* **14** 501–518.

Peterson JJ. 1972. Calculations of sulfur dioxide concentrations over metropolitan St. Louis. *Atmospheric Environment* **16**: 433–442.

Sasaki Y. 1960. An objective analysis for determining initial conditions for the primitive equations. Techniical Report. Ref. 60-16T, (Texas A/M University College Station.,

Şen Z. 1989. Cumulative semivariogram models of regionalized variables. *Math. Geol.* **21**: 891–903.

Şen Z. 1995. Regional air pollution assessment by cumulative semivariogram technique. *Atmospheric Environment* **29**: 543–458.

Taylor GI. 1915. Eddy motion in the atmosphere. *Phil. Trans. Roy. Soc., A* **215**: 1.

Taylor JA, Jakeman AJ, Simpson RW. 1986. Modeling distributions of air pollutant concentrations–I. Identification of statistical models. *Atmospheric Environment* **20**: 1781–1789.

Zinsmeister AR, Redman TC. 1980. A time series analysis of aerosol composition measurements. *Atmospheric Environment* **14**: 201–215.

